Journal of Alloys and Compounds, 194 (1993) 287–294
JALCOM 7201

Mechanical milling of ordered intermetallic compounds: the role of defects in amorphization

Y. S. Cho and C. C. Koch
Materials Science and Engineering Department, North Carolina State University, Raleigh, NC 27695–7907 (USA)

(Received February 11, 1992; in final form April 9, 1992)

Abstract

The role of defects in the amorphization of ordered intermetallic compounds by high energy ball milling was addressed. The structural evolution with milling time was studied experimentally in the intermetallic compounds Ni_3Si and CoZr. The results of these studies were compared with previous work on Ni_3Al and Nb_3Sn. In these four compounds, the significant contributions to stored energy come from two major sources: (1) anti-site disorder $\Delta G^{\text{disorder}}$, and (2) grain boundary energy of nanoscale grains $\Delta G^{\text{grain boundary}}$. The occurrence, or not, of amorphization by ball milling was consistent with estimated values of free energy such that $\Delta G^{\text{disorder}} + \Delta G^{\text{grain boundary}} \geqslant \Delta G^{\text{a-c}}$ where $\Delta G^{\text{a-c}}$ is the difference in free energy between the ordered crystalline and amorphous phases. While the accuracy of the estimated ΔG values is quite variable, the values are consistent with the results. For Ni_3Si no amorphization was observed and $\Delta G^{\text{disorder}} + \Delta G^{\text{grain boundary}} < \Delta G^{\text{a-c}}$. In the cases of Ni_3Al which exhibited partial amorphization, and Nb_3Sn which was completely amorphized, $\Delta G^{\text{disorder}} + \Delta G^{\text{grain boundary}} \geqslant \Delta G^{\text{a-c}}$. For CoZr which was completely amorphized, both $\Delta G^{\text{disorder}} > \Delta G^{\text{a-c}}$ and $\Delta G^{\text{grain boundary}} > \Delta G^{\text{a-c}}$. Since no disordering of CoZr was observed experimentally, it is concluded that the nanoscale grain boundaries drive the amorphization reaction in ordered CoZr.

1. Introduction

There has been considerable interest in recent years in the synthesis of amorphous structures by high-energy ball-milling of either elemental powder mixtures [1] or powders of intermetallics [2]. In the case of amorphization of intermetallics, defects introduced by the deformation during milling must be responsible for raising the free energy of the crystalline compound to that of the amorphous phase. The critical question in this regard is: what defects can provide the required increase in free energy? While free energy differences between the crystalline compound and the amorphous alloy are typically 5–20 kJ mol^{-1}, the stored energy of deformation from conventional deformation processes is rarely more than about 1–2 kJ mol^{-1} or less than or equal to 5% of the heat of fusion [3]. A maximum value for the stored energy associated with a very high dislocation density of about 10^{14} cm^{-2} in cold-rolled NiTi was estimated to be 2.2 kJ mol^{-1} by Koike *et al.* [4]. Amorphization in intermetallics by the plastic deformation supplied by ball milling is analogous to amorphization in intermetallics by irradiation with energetic particles such as electrons, ions, or neutrons. Luzzi and Meshii [5] have reviewed experimental evidence that suggests that the energy increase due to chemical anti-site disordering is the major driving force behind the electron-irradiation induced amorphization in intermetallic compounds. It is likely that anti-site disordering can provide sufficient energy for amorphization of intermetallics by milling in some cases. Seki and Johnson [6] have suggested that the amorphization of the $CuTi_2$ intermetallic by ball milling was driven mainly by the energy stored in antiphase domain boundaries. Contributions from dislocations and grain boundaries were estimated to be 1 kJ mol^{-1} and 1.6–2.9 kJ mol^{-1} respectively. The remainder of the stored energy required for amorphization (the enthalpy of crystallization $=11$ kJ mol^{-1}) was believed to come from the disordering at antiphase boundaries. Bakker and coworkers [7, 8] have argued that anti-site chemical disorder is the main source of energy storage in ball-milled intermetallics. They suggest that amorphization results if the free energy of the disordered compound exceeds the free energy of the amorphous state. However, Jang and Koch [9] observed the long-range order (LRO) parameter to decrease to zero at milling times a factor of ten shorter than the time at which partial amorphization was first observed in Ni_3Al. Similarly, Cho and Koch [10] determined that the LRO in ball-milled Nb_3Sn disappeared after about 1 h of milling while amorphization was not initiated until 5–6 h of milling.

0925-8388/93/$6.00

It was suggested that the additional stored energy required for the crystalline-to-amorphous transformation in Nb_3Sn came from the grain boundary energy of the fine nanocrystalline grain structure that evolved during milling of the disordered compound. However, only partial amorphization was observed in Ni_3Al so quantitative comparisons of the energy terms were not possible. Also, amorphous Nb_3Sn crystallizes at temperatures (approximately 750–800 °C) just above the temperature range (725 °C) of our differential scanning calorimetry (DSC) equipment so that quantitative values for the enthalpy of crystallization were not obtained.

Thus, in order to study further the role of anti-site disorder and nanocrystalline grain boundaries in amorphization of intermetallics by milling, two other intermetallics were chosen in the present work. The CoZr intermetallic has the ordered b.c.c., B2 crystal structure, is known to amorphize completely by mechanical milling [11], and crystallizes below 725 °C [12]. The Ni_3Si intermetallic has the ordered f.c.c., Ll_2 crystal structure and does not amorphize by ball milling but forms a fine nanocrystalline grain structure [13]. A comparison of the evolution of the structural changes with milling time in these intermetallics which exhibit amorphization (CoZr) or not (Ni_3Si) will be presented along with estimates of the relevant free energy contributions. Comparisons will be made with the published results on Ni_3Al and Nb_3Sn referred to above.

2. Experimental procedure

The intermetallic Ni_3Si and CoZr compounds were prepared by arc-melting the pure components in a partial pressure of titanium or zirconium gettered argon on a water-cooled copper hearth. In order to ensure the homogeneity of the intermetallic compounds, the arc-melted buttons were remelted at least four times and then annealed for 3–5 h at 850 °C under a vacuum of 1.3×10^{-5} Pa. The annealed buttons were crushed to powders in a mortar and pestle. Before mechanical milling, powders were annealed for 2 h at 800 °C under a vacuum of 1.3×10^{-5} Pa to anneal out the plastic deformation introduced during crushing and maximize the LRO. Ni_3Si powders were milled in a Spex Mixer/Mill (model 8000) and the CoZr compound in an Invicta vibratory mill (model BX920/2). Milling was performed in both devices with a hardened tool-steel vial and martensitic stainless-steel balls. The powders were charged into the vial in an argon-filled glove box. The vial with an elastimer O-ring seal was tightly closed after flushing with argon gas. The weight ratio of ball to powder was 10:1 for the Spex mill (SM) with a ball diameter of 7.9 mm and for the less energetic vibratory mill (VM) various sizes of balls were used with the weight ratio of 45:1 to decrease the milling time. Mechanically milled powders were characterized by X-ray diffraction measurements in a GE XRD-5 diffractometer with a graphite monochromator. Cu Kα radiation (wavelength 0.15418 nm) was used for the Ni_3Si compound and Co Kα (wavelength 0.179 nm) radiation for the CoZr compounds. In addition, CoZr was also studied in a Rigaku diffractometer with Cu Kα radiation and a graphite monochrometor. From X-ray diffraction, the grain size was estimated by the Scherrer equation from the measured line broadening, and the LRO parameter was calculated by comparing the intensities of the fundamental and the superlattice lines. The thermal stability of the amorphous or disordered structures of milled Ni_3Si and CoZr powders was examined in a computerized differential scanning calorimeter (Du Pont model 9900) in a purified argon atmosphere. The microstructural evolution during milling was followed with transmission electron microscopy (TEM) in a Hitachi-800 microscope operating at 200 kV. Specimens for TEM were prepared by compressing the powder under a pressure of 3 GPa into a disk with 3 mm diameter and thickness of 60–100 μm. The compacted disc was mechanically dimpled and then ion milled in a Gatan Model 600 ion miller. Oxygen analyses were made at Teledyne Wah-Chang Albany Company using the inert-gas fusion technique.

3. Results

3.1. Milling of Ll_2Ni_3Si powder

The intermetallic Ni_3Si compound was milled in a Spex-shaker mill at room temperature. Ni_3Si has the Ll_2 (ordered f.c.c., *i.e.* $AuCu_3$ type) structure. The initial, ordered Ni_3Si compound clearly reveals the superlattice lines (mixed *hkl* indices, *e.g.* (100), (110), (210) and (211) etc.) by X-ray diffraction, as shown in Fig. 1. After a short milling time (i.e. 1 h), all the superlattice lines disappear, indicating that the ordered Ni_3Si becomes fully disordered. The LRO parameter S was calculated by comparing the intensities of the fundamental and the superlattice lines. The annealed Ni_3Si powder before milling has an S value of 0.96. The S values decrease monotonically with milling time and the ordered Ll_2 structure becomes completely disordered, *i.e.* $S=0$, after 1 h milling, as shown in Fig. 2. The X-ray diffraction pattern at the longest milling time of 80 h exhibits broad crystalline f.c.c. peaks, indicating that Ni_3Si can be disordered but cannot be amorphized by mechanical milling. The grain size of Ni_3Si powders as a function of milling time, as calculated by the Scherrer formula from the X-ray line broadening decreases with milling time. The "grain" size of about 1 μm before milling drastically decreased to a size of

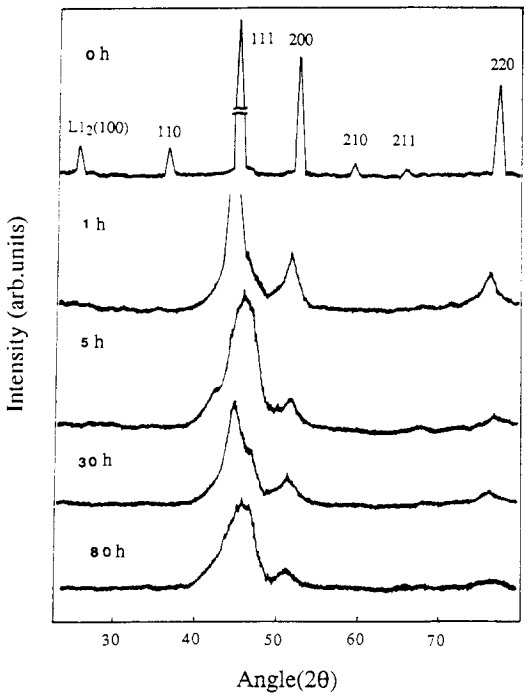

Fig. 1. X-ray diffraction patterns of Ni_3Si for various milling times, Cu Kα radiation.

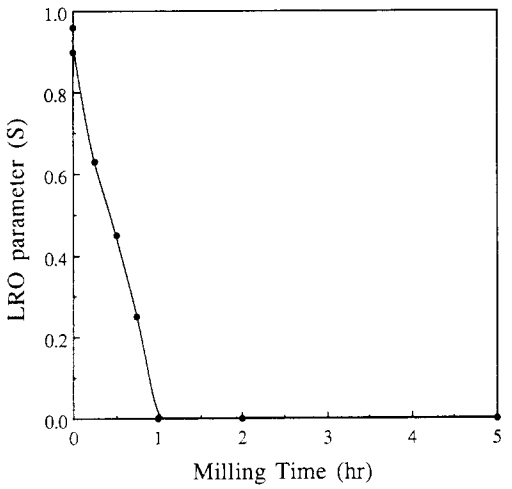

Fig. 2. Long-range-order parameter S *vs.* milling time for Ni_3Si.

less than 100 nm after 0.5 h of milling and then decreased to about 15 nm after 50 h and saturated to a constant value of about 8–12 nm at 80 h. The grain size estimated by X-ray diffraction line broadening is somewhat smaller than that observed by TEM at intermediate milling times. This is presumably because we did not take account of instrumental line broadening or the strain contribution to line broadening. At a final milling time of 80 h, the grain sizes of about 8–12 nm determined by both the methods are in good agreement.

TEM was used for the microstructural study. At early milling times, *e.g.* 0.25 h, dislocation cell structures were observed with cell diameters of 100–300 nm. A bright-field TEM image illustrating the dislocation cell structure for Ni_3Si milled for 0.25 h is shown in Fig. 3. The absence of the superlattice reflections in the selected area diffraction (SAD) pattern indicates that this region is fully disordered owing to heavy deformation provided by milling although the LRO parameter at this milling stage is 0.64 as determined macroscopically by X-ray diffraction, Fig. 2. The cell boundaries sharpened and the cells become smaller with milling time. By 5 h of milling, the grain size dropped to an average of 15 nm, as shown in Fig. 4(a) which is the typical area observed at this milling time; however, a nanocrystalline region was also observed. That is, the microstructure was inhomogeneous at this stage. This is shown in Fig. 4(b) for which the insets A and B are the corresponding SAD patterns of the regions A and B respectively. The grain size in region A is about 8 nm. As milling continues to 80 h, only the nanocrystalline grain structure was observed by TEM, as Fig. 5 illustrates. The grain diameter ranges from 8 to 12 nm. However, there were no amorphous regions detected by TEM or X-ray diffraction for the longest milling times and milling longer (*e.g.* 100 h) did not change the microstructure.

The enthalpy change measured by DSC is plotted in Fig. 6 as a function of milling time. The enthalpy increased very rapidly up to 5 h milling time and then saturated at a value of about 10 kJ mol^{-1}. It has been reported [14] that atomic order in $L1_2$ Ni_3Si is not thermally affected up to the melting temperature and it is difficult to disorder the ordered Ni_3Si by conventional means, *e.g.* quenching. The formation of disordered Ni_3Si has, however, been observed during implantation of silicon onto nickel at a temperature of 400 °C or below [15]. At the milling time of 1 h when the ordered $L1_2$ Ni_3Si becomes disordered, the onset temperature for the disorder-to-order transition is 406

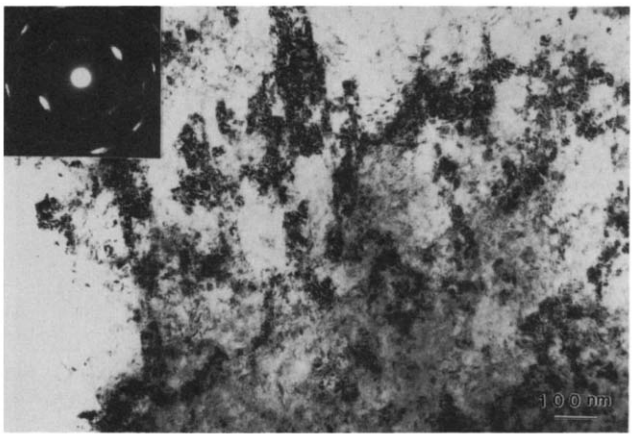

Fig. 3. TEM image and SAD pattern for Ni_3Si milled for 0.25 h showing dislocation cell structure.

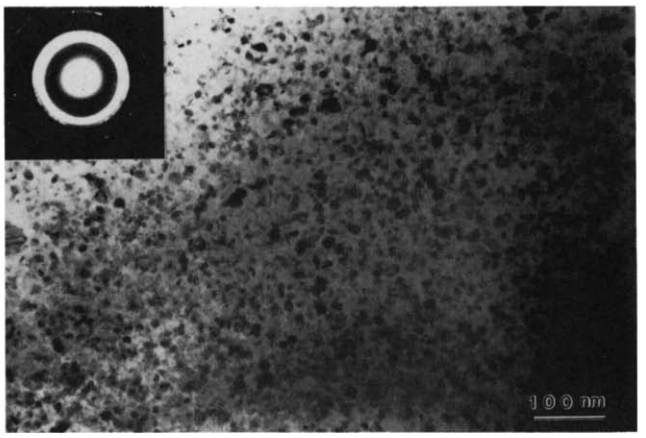

(a)

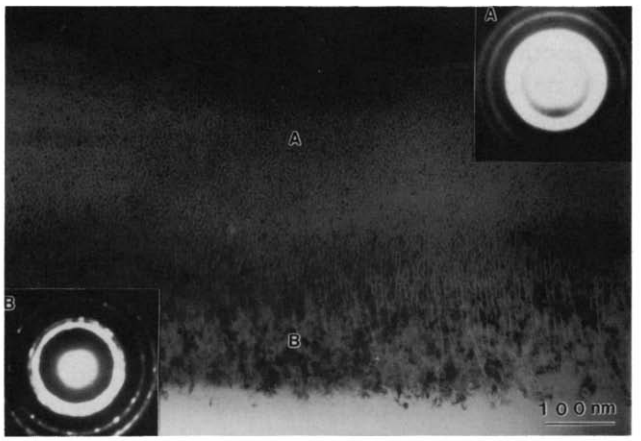

(b)

Fig. 4. (a) TEM image and SAD pattern for Ni_3Si milled for 5 h; typical region, grain sizes of 10–25 nm. (b) TEM image and SAD patterns for Ni_3Si milled for 5 h; inhomogeneous grain size region, nanocrystalline grains in region A with about 8 nm diameters.

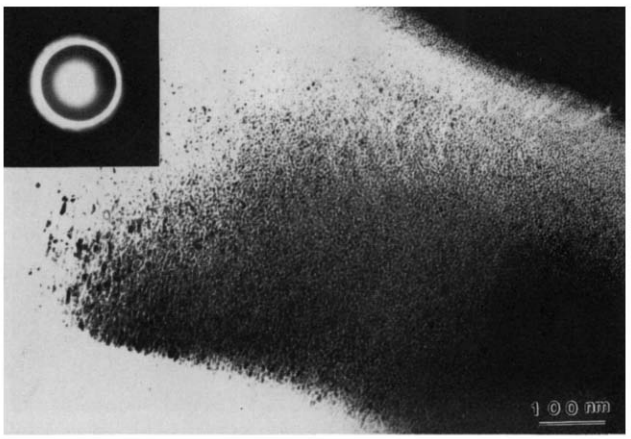

Fig. 5. TEM image and SAD pattern for Ni_3Si milled for 80 h.

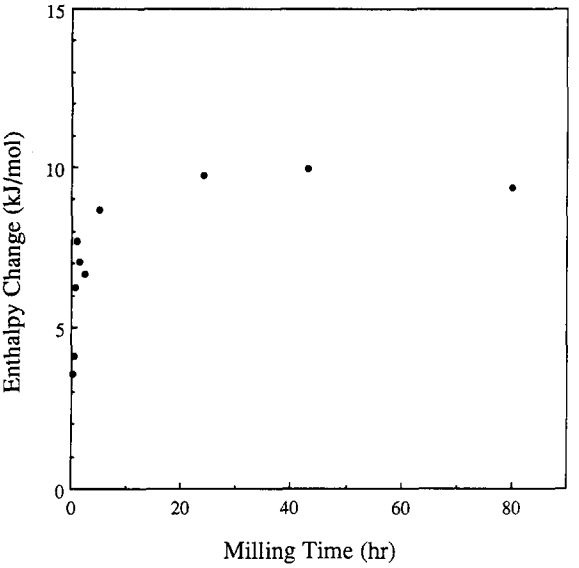

Fig. 6. Enthalpy change ΔH for exothermic peak in DSC as a function of milling time for Ni_3Si.

°C which agrees very well with the ordering temperature of about 400 °C, as mentioned above. During the disorder-to-order transition, the enthalpy change measured by DSC is 5.6 kJ mol^{-1} which is close to the ordering energy (5 kJ mol^{-1}) calculated by Potter [16].

3.2. *Milling of B2 CoZr compound*

CoZr compound was milled in a vibrating-mill at room temperature with a ball-to-powder weight ratio of 45:1. Since B2 CoZr is a line compound it is relatively difficult to obtain a single phase by conventional arc-melting and solidification. The CoZr powders prepared by arc-melting and annealing were not a single phase, *i.e.* they contained a small amount of Co_2Zr. Figure 7 presents the X-ray diffraction patterns as a function of milling time. The X-ray diffraction of unmilled powder shows the diffraction lines from the Co_2Zr phase. CoZr has an ordered b.c.c. structure (CsCl type) and the superlattice lines are those which have an odd number for $h+k+l$ indices (*e.g.* 100, 111, 210...). The LRO parameter S was calculated by comparing the intensities of the superlattice (*e.g.* (100)) and the fundamental (*e.g.* (110)) lines and was found to be 0.96 ± 0.04 for the annealed unmilled powder. No decrease in the value of S was observed with milling time to within experimental accuracy. A broad amorphous peak appears as the milling time increases and is clearly evident after 24 h of milling along with the broadened fundamental and superlattice lines. The relative intensities of the superlattice *vs.* fundamental lines do not show any change at this stage when the amorphous phase is also present and $S \approx 1$ to experimental accuracy. After further milling the crystalline lines become weaker with respect to the amorphous peak and finally after 80 h

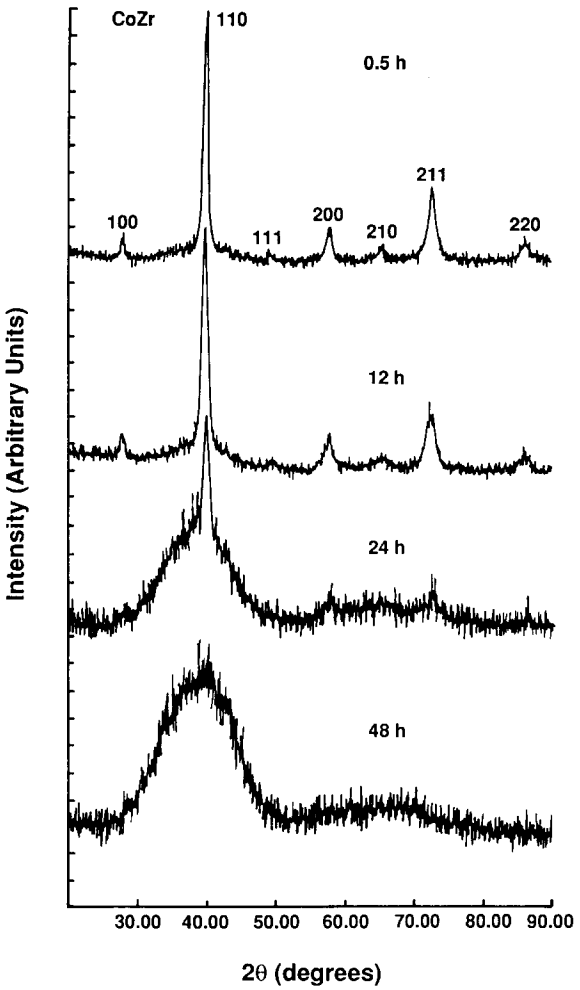

Fig. 7. X-ray diffraction patterns of CoZr for various milling times, Cu Kα radiation.

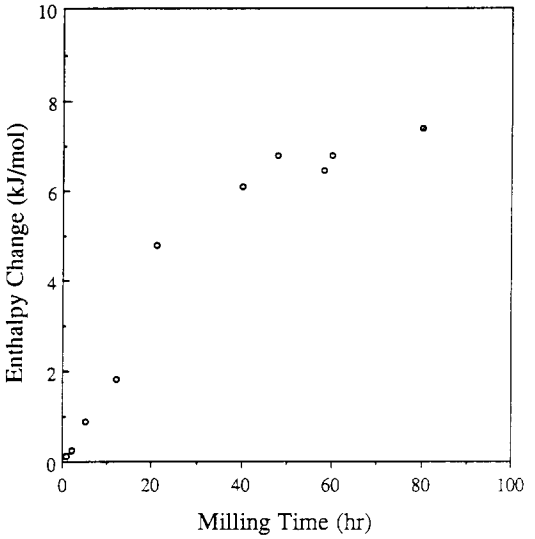

Fig. 8. Enthalpy change ΔH for exhermic peak in DSC as a function of milling time for CoZr.

of milling the diffraction pattern appears to be that of an essentially completely amorphous structure.

The change in grain size of CoZr during milling was estimated using the Scherrer formula. The average grain size decreased rapidly during the early milling times, for example it dropped to 20–30 nm after 5 h of milling. The apparent grain size decreased to a constant value of about 4–6 nm after 21 h of milling.

The enthalpy change during milling as measured by DSC is shown in Fig. 8 as a function of milling time. After 80 h of milling, when an amorphous X-ray diffraction pattern is evident, the measured enthalpy is 7.5 kJ mol^{-1}. This may be compared with the crystallization enthalpy of CoZr metallic glass ribbon prepared by melt-spinning of 7.8 kJ mol^{-1} [17]. The agreement is very good.

The oxygen contents of milled Ni_3Si and CoZr powders were determined to increase with milling time but were never greater than about 5000 ppm at the longest milling times studied. These levels of oxygen contamination do not appear to affect the amorphization process.

4. Discussion

4.1. Ni_3Si

Milling the ordered Ll_2 intermetallic compound Ni_3Si resulted in the following sequence of structural changes: ordered Ll_2 structure → disordered f.c.c. with dislocation cell structure → nanocrystalline f.c.c. structure. This evolution of the structure of Ni_3Si with milling time has also been observed recently by Jang and Tsau [18]. Their results agree qualitatively with ours, but there are some quantitative differences although they used the same nominal milling conditions. They observe complete disordering after 2 h milling compared with 1 h in our case and a maximum measured enthalpy for the exothermic peak observed using DSC at about 430 °C of 15.5 kJ mol^{-1} compared with about 10.0 kJ mol^{-1} in the present work. Similarly, the enthalpy release for the milling time where complete disordering occurs is 11 kJ mol^{-1} compared with about 5.5 kJ mol^{-1} in the present work. The compositions of our samples are slightly different, ours are 25 at.% silicon, whereas the Jang and Tsau samples are 24 at.% silicon meaning that we have a larger trace amount of the Ni_5Si_2 second phase. They claim oxygen contents of less than 0.4 at.% while we measure 1.5 at.% oxygen for the longest milling times of 80 h. It seems unlikely that these small differences in composition could be the cause of the quantitative differences in enthalpy reported.

Jang and Tsau also calculate the difference in free energies between ordered Ll_2 and amorphous Ni_3Si.

Their estimation, based on a combination of approximations including Miedema's model [19], appears to be much larger (50 kJ mol^{-1}) than our estimates which incorporate data inputs for heat of formation and give values ranging from 10.5 to 21.5 kJ mol^{-1}. Since there are no experimental crystallization enthalpy data to compare with, we cannot confirm which estimate is more correct. However, if one uses a modified Richards rule [20] one obtains 17.9 kJ mol^{-1} for the heat of fusion of Ni_3Si. Since ΔH^{cryst} must be smaller than ΔH^{fusion}, if this estimate is correct, our lower values are more consistent. While the quantitative agreement with the results of Jang and Tsau is not good the same qualitative conclusions are reached. That is, in the case of Ni_3Si, the combination of disordering energy and the energy supplied by the nanocrystalline grain boundaries is not sufficient to overcome the energy difference between ordered Ll_2 Ni_3Si and amorphous Ni_3Si. Therefore, amorphization by mechanical attrition is not observed in this compound.

4.2. CoZr

The amorphization by milling of CoZr is in direct contrast to the above results on Ni_3Si. The CoZr intermetallic compound can be completely amorphized by ball milling. We also have more accurate values in the case of CoZr for the relevant defect energies and the energy difference between the ordered intermetallic and the amorphous phases. The experimental crystallization enthalpy for amorphous CoZr prepared by rapid solidification (melt spinning) is 7.8 kJ mol^{-1} [17] which compares closely with our value of 7.5 kJ mol^{-1} for the enthalpy of our sample milled for 80 h which appears to be almost completely amorphous. The free energy difference between the ordered crystalline and amorphous phases can then be estimated by including the entropy of mixing for an ideal solution ($\Delta S_{mix} = R(x_A \ln x_A + x_B \ln x_B)$). This gives a value for ΔG^{a-c} of 5.8 kJ mol^{-1} at 350 K. This is consistent with the calculations of Gärtner and Bormann [21] who used experimental data in conjunction with the CALPHAD method. They obtained a value for ΔG^{a-c} of about 6.0 kJ mol^{-1} at 723 K. If we approximate the temperature dependence of ΔG^{a-c} by the expression of Singh and Holz [22] we obtain a value of 6.5 kJ mol^{-1} at 350 K. Similarly, Gärtner and Bormann [21] calculated the free energy difference at 723 K between ordered CoZr and disordered (b.c.c.) CoZr to be about 22.0 kJ mol^{-1}. The calculation for the energy contribution from the nanocrystalline grain boundaries is less precise. We assumed cubic grains to calculate the grain boundary area per mole. The "grain size" was defined as 1.209 × cube side as the "mean tangent diameter" for a sphere of equal volume [23]. The grain boundary energies are for the most part unknown but a range of energies from 1000 mJ m^{-2} to 1400 mJ m^{-2} was used, consistent with the grain boundary energies calculated by computer simulation for Ni_3Al [24]. To test this procedure we used the experimental data for nanocrystalline iron of Fecht *et al.* [25] where an enthalpy of 2.0 kJ mol^{-1} was measured for an 8 nm average grain size. We used the literature value for the grain boundary energy of α-iron, 760 mJ m^{-2} [26], and obtained a value of 2.4 kJ mol^{-1} for cubic grains 8 nm/1.209 per cube side. This reasonable agreement with the experimental result gives us some confidence in the procedure. In Fig. 9 the calculated total grain boundary energy for CoZr is plotted against grain size in the nanocrystalline regime. The range of values was determined as follows: (1) the low value used 1000 mJ m^{-2} as the specific grain boundary energy and normalized to the above result on iron; (2) the high value was 1400 mJ m^{-2} as the specific grain boundary energy. The difference in free energy between ordered CoZr and amorphous CoZr is also plotted. The intersection of these curves suggests that nanocrystalline grain sizes in the range of about 5–8 nm could supply the free energy difference to drive the crystalline-to-amorphous phase transformation in

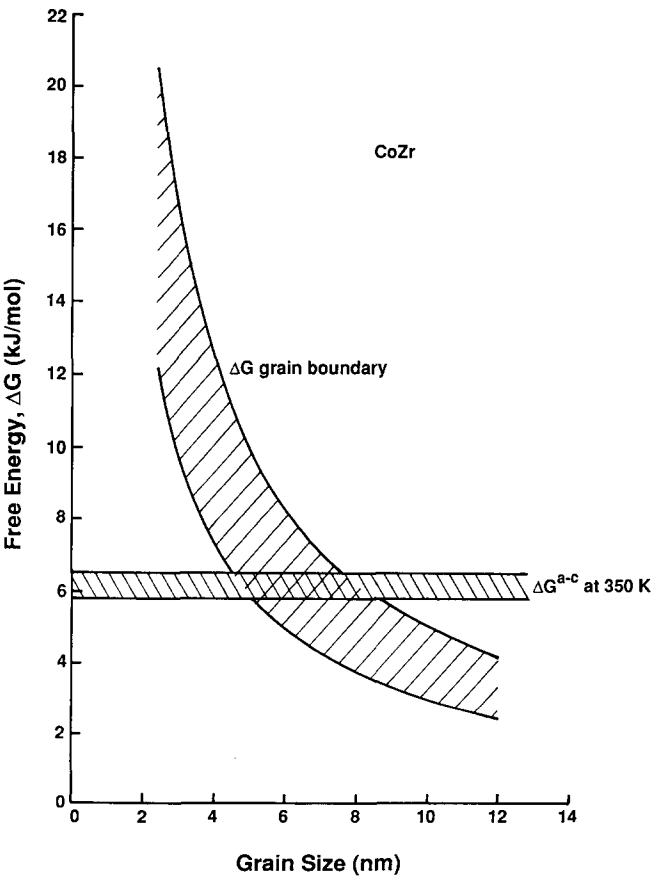

Fig. 9. Grain boundary energy, $\Delta G^{grain\ boundary}$, as a function of nanocrystalline grain size for CoZr along with the free energy difference, ΔG^{a-c}, between ordered crystalline CoZr and amorphous CoZr.

CoZr. While both the energy of anti-site disordering (22 kJ mol^{-1}) and of the nanocrystalline grain boundaries (5–10 kJ mol^{-1}) are sufficient to drive the amorphization in CoZr, since no evidence of disordering is observed by X-ray diffraction up to the milling times when amorphization occurs, it is the nanocrystalline grain boundaries that are responsible. It appears that the ordered phase of CoZr is very stable with respect to the disordered b.c.c. phase, as illustrated by the calculations of Gärtner and Bormann [21] and plastic deformation provides the defect energy to drive the amorphization via the creation of the nanocrystalline grain boundaries as opposed to anti-site disorder.

4.3. *Defect energies and amorphization for the ordered intermetallics Ni_3Si, Ni_3Al, Nb_3Sn and CoZr*

The structural evolution with milling time was studied in Ni_3Si, Ni_3Al, Nb_3Sn, and CoZr. Table 1 summarizes the structural changes observed, gives estimates of the free energy differences between the crystalline and amorphous phases, and provides estimates for the anti-site disordering energy and the nanocrystalline grain boundary energy. These estimates vary in reliability from relatively high for CoZr where experimental data and CALPHAD calculations are available, to low for Nb_3Sn where estimates based on a modified Richard's Rule [20] are the only available approximations for the energy differences between the ordered crystalline and amorphous phases. The estimates for the anti-site disordering energies were taken from either the enthalpy observed using DSC at milling times when disorder was complete, taken as 21%–37% of the enthalpy of formation [5, 19], or from CALPHAD calculations [21]. Enthalpies were converted to free energies by calculating the entropy of mixing for the ideal solution at 350 K as described above. Nanocrystalline grain boundary energies were estimated from the observed grain sizes using the procedure outlined earlier in this paper.

We can draw the following conclusions from the data summarized in Table 1. In spite of the large variations in the estimates for the various energy terms the results can be summarized for the compounds studied.

(1) *Ni_3Si.* The sum of the anti-site disordering energy and the grain boundary energy is not sufficient to overcome the energy difference between the ordered crystalline and amorphous phases. This is consistent with no observation of amorphization.

(2) *Ni_3Al.* The sum of the anti-site disordering energy and the grain boundary energy is comparable with or greater than ΔG^{a-c}. However, since only partial amorphization is observed in Ni_3Al, the accuracy of these energy values is suspect.

(3) *Nb_3Sn.* The sum of $\Delta G^{\text{disordering}}$ and $\Delta G^{\text{grain boundary}}$ is comparable with ΔG^{a-c}. Complete amorphization is observed at milling times about five times longer than those where disordering is complete. These observations are consistent with the driving free energy for the crystalline-to-amorphous phase transformation as the sum of the disordering and grain boundary energies.

(4) *CoZr.* Both $\Delta G^{\text{disordering}}$ and $\Delta G^{\text{grain boundary}}$ are large for CoZr and individually can overcome ΔG^{a-c}. Since no experimental evidence exists for disordering (*i.e.* $S \approx 1.0$) up to and beyond the milling times when amorphization begins, it is concluded that the creation of the fine nanocrystalline grains in perfectly ordered CoZr drives the phase transformation. Detailed microstructural evidence is needed to confirm this conclusion which is based upon X-ray diffraction measurements.

TABLE 1. Estimated free energy contributions to the crystalline → amorphous transformation energy from anti-site disorder and nanocrystalline grain boundaries for Ni_3Si, Ni_3Al, Nb_3Sn and CoZr

Compound	Anti-site disorder (kJ mol^{-1})	Nanocrystalline grain boundaries (kJ mol^{-1})	ΔG, crystalline to amorphous (kJ mol^{-1})	Amorphization
Ni_3Si	3.9[a] 3.9–11.7[b] 5.0 (ref. 16)	3.0 (for 10 nm grain diameter)	10.5–21.5 50.0 (ref. 18) 7.4[c]	No
Ni_3Al	5.3–10.6[b] 6.4[a]	4.0 (6 nm diameter) 11.6 (2 nm diameter)	10–12 (ref. 27) 8.8[c]	Partial
Nb_3Sn	1.8–4.3[b]	6.7 (6 nm diameter) 8.2 (5 nm diameter)	13.4[c]	Yes
CoZr	22.0 (ref. 21) 6.8–13.5[b]	4.9–8.2 (6 nm diameter) 5.9–10.0 (5 nm diameter)	5.8 (ref. 17) 6.5 (ref. 21) 8.3[c]	Yes

[a]From DSC at milling time when $S = > 0$ corrected by entropy of mixing at 350 K.
[b]21%–37% of enthalpy of formation corrected by entropy of mixing at 350 K.
[c]Modified Richard rule [20], assuming $\Delta G^{c-a} = \frac{1}{2} \Delta H^{\text{fusion}}$, corrected to ΔG by entropy of mixing at 350 K.

5. Summary

The structural evolution with milling time was followed in the intermetallic compounds Ni_3Si and CoZr. The results of these studies were compared with previous work on Ni_3Al and Nb_3Sn. In all these ordered intermetallic compounds, significant contributions to stored energy come from two major sources: (1) antisite disorder, and (2) grain boundary energy of nanoscale grains. The occurrence or not of amorphization by ball milling was consistent with the values of free energy estimated such that $\Delta G^{\text{disorder}} + \Delta G^{\text{grain boundary}} \geqslant \Delta G^{\text{a-c}}$. For Ni_3Si, $\Delta G^{\text{disorder}} + \Delta G^{\text{grain boundary}} < \Delta G^{\text{a-c}}$ and no amorphization was observed. In Ni_3Al and Nb_3Sn complete disordering occurs at milling times well before any amorphous phase appears so the combination of $\Delta G^{\text{disorder}} + \Delta G^{\text{grain boundary}}$ is necessary to induce partial amorphization in Ni_3Al and complete amorphization in Nb_3Sn. In CoZr, $\Delta G^{\text{disorder}} > \Delta G^{\text{a-c}}$ and also $\Delta G^{\text{grain boundary}} \geqslant \Delta G^{\text{a-c}}$. Since no decrease in LRO for CoZr from $S \approx 1.0$ was observed at milling times when amorphization began, it is concluded that the creation of the nanocrystalline grains in ordered CoZr is responsible for the amorphization transformation.

Acknowledgments

The authors wish to thank D. Pathak for assistance with the experimental work. This research was supported by the National Science Foundation under Grant No. DMR-8620394-02.

References

1 C. C. Koch, O. B. Cavin, C. G. McKamey and J. O. Scarbrough, *Appl. Phys. Lett., 43* (1983) 1017.
2 R. B. Schwarz and C. C. Koch, *Appl. Phys. Lett., 49* (1986) 146.
3 M. B. Bever, D. L. Holt and A. L. Titchener, *Prog. Mater. Sci., 17* (1973) 1.
4 J. Koike, D. M. Parkin and M. Nastasi, *J. Mater. Res., 5* (1990) 1414.
5 D. E. Luzzi and M. Meshii, *Res. Mech., 21* (1987) 207.
6 Y. Seki and W. L. Johnson, in A. H. Clauer and J. J. deBarbadillo (eds.), *Solid State Powder Processing,* TMS, Warrendale, PA, 1990, pp. 287–297.
7 D. L. Beke, H. Bakker and P. I. Loeff, *Coll. Phys. C4, 14* (1990) C4-63.
8 H. Bakker and L. M. Di, in P. H. Shingu (ed.), *Proc. Int. Symp. on Mechanical Alloying, May 1991, Kyoto, Trans. Tech.,* 1992, p. 27.
9 J. S. C. Jang and C. C. Koch, *J. Mater. Res., 5* (1990) 498.
10 Y. S. Cho and C. C. Koch, *Mater. Sci. Eng., A141* (1991) 139.
11 A. W. Weeber and H. Bakker, *Proc. LAM6 Conf., Garmisch-Partenkirchen, 1986,* Vol. 2, Oldenburg, Munich, 1987, p. 221.
12 K. H. J. Buschow, *J. Phys. F, 14* (1984) 593.
13 C. C. Koch and Y. S. Cho, *Nanostructured Mater., 1* (1992) 207.
14 D. Franks and H. Jang, *MRS Symp. Proc., 81* (1987) 65.
15 S. G. B. Mayer, F. F. Milillo and D. I. Potter, *MRS Symp. Proc., 39* (1985) 521.
16 D. I. Potter, in R. Holland, L. Mansur and D. I. Potter (eds.), *Phase Stability During Irradiation,* TMS-AIME, Warrendale, PA, 1981, p. 521.
17 Z. Altounian, R. J. Shank and J. O. Strom-Olsen, *J. Appl. Phys., 58* (1985) 1192.
18 J. S. C. Jang and C. H. Tsau, submitted to *J. Mater. Sci.*
19 F. R. de Beer, R. Boom, W. C. M. Mattens, A. R. Miedema and A. K. Niessen, *Cohesion in Metals, Transition Metal Alloys,* North-Holland, Amsterdam, 1988.
20 D. Goodman, J. W. Cahn and L. H. Bennett, *Bull. Alloy Phase Diagrams, 2* (1981) 29.
21 F. Gärtner and R. Bormann, *Collo. Phys. C4, 51* (1990) C4–95.
22 H. B. Singh and A. Holz, *Solid State Commun., 45* (1983) 985.
23 J. E. Hilliard, in H. Elias (ed.), *Stereology,* Springer, New York, 1968, p. 211.
24 S. P. Chen, D. J. Srolovitz and A. F. Voter, *J. Mater. Res., 4* (1989) 62.
25 H. J. Fecht, E. Hellstern, Z. Fu and W. L. Johnson, *Metall. Trans. A, 21* (1990) 2333.
26 L. H. Van Vlack, *J. Met., 3* (1951) 25.
27 R. Bormann, CALPHAD calculation, personal communication, 1990.